Proceedings of the ASME 2014 Internal Combustion Engine Division Fall Technical Conference

ICEF2014

October 19-22, 2014, Columbus, IN, USA

ICEF2014-5459

Effects of Injection Pressure on Combustion, Nanoparticles and Gaseous Emissions Characteristics from a Common-Rail HSDI Diesel Engine running on ULSD and RME

Hayder A. Dhahad
Mechanical Engineering Department
University of Technology, Baghdad, Iraq

Mohammed A. Abdulhadi
Mechanical Engineering Department
University of Technology, Baghdad, Iraq

Ekhlas M. Alfayyadh
Mechanical Engineering Department
University of Technology, Baghdad, Iraq

T. Megaritis
Centre for Advanced Powertrain and Fuels Research
School of Engineering and Design, Brunel University,
London, UK

ABSTRACT

In this paper the effect of injection pressure on combustion characteristics (including apparent heat release rate, ignition delay, combustion duration and relative quantities of premixed and diffusion combustion), pollutant emissions (NO_x, CO and THC), smoke number and nanoparticle emissions are reported. The following experiment was performed using a high speed direct injection (HSDI) diesel engine fueled with ultra-low sulfur diesel (ULSD) and rapeseed methyl esters (RME), running at a constant speed (1500 rpm) and at constant fuel injection timing (-9 ATDC). Injection pressures of 800, 1000 and 1200 bar were tested, at two engine loads (2.5 and 5 bar BMEP). NO_x, CO and THC were measured using a Horiba-Mexa 7170DEGR gas analyser. An electrostatic mobility spectrometer (EMS) was used in this experiment to obtain exhaust soot particle number size distributions, and smoke number (SN) was measured using an AVL–415 smoke meter. It was found that when the injection pressure was increased the ignition delay was reduced, leading to an advance in combustion, and increases in in-cylinder pressures and heat release rates. Combustion was further advanced when fueling on RME, since the fuel exhibited a shorter ignition delay. The premixed burn fraction increased with fuel injection pressure, and this was associated with a decrease in exhaust SN, THC and CO emissions, but an increase in NO_x emissions. At low load NO_x and CO emissions generated by RME were less than those generated by USLD. Conversely, at high load RME generated higher NO_x, CO and THC. USLD generated more soot than RME at high load and slightly less at low load. The nanoparticles size distribution curves were all unimodal in shape and most of the measured particles were in the range of 5-100 nm in diameter. The nucleation particle numbers have shown to be higher for RME biodiesel at all engine operating conditions and accumulation mode particles are higher for ULSD.

1. Introduction

Biodiesel, as an alternative fuel for internal combustion engines, is attracting increasing attention worldwide, and is defined as a mixture of fatty acid methyl or ethyl esters derived from a renewable lipid feedstock, such as vegetable oil or animal fat, and can be used pure or in blends with petroleum diesel fuel [1-3] . Biodiesel fuel has many effects on diesel engine emissions. A large amount of studies have been conducted on the properties of biodiesel and emissions generated by its use. Dwivedi et.al [4] conducted a review of the impact of the use of biofuels on engine performance and exhaust emissions. Biodiesel is much more suitable for use as an engine fuel than straight vegetable oil for a number of reasons, the most notable one being its lower viscosity. Furthermore, there is a substantial body of evidence showing that the use of biodiesel (and biodiesel blends) has a strong and consistent beneficial effect on the emissions of hydrocarbons (THC), carbon monoxide (CO), and particulate matter (PM) [5], while the effects of biodiesel are smaller and more variable for NO_x emissions, although generally NO_x increases slightly with the use of biodiesel. The biodiesel NO_x effect can be mitigated by modifying engine control settings, particularly by retarding injection timing and increasing exhaust gas recirculation (EGR). The absolute magnitude of the biodiesel NO_x effect appears to be reduced with modern engines, although there are cases where the percentage change is still substantial [6].

In the exhaust from diesel engines, PM primarily consists of agglomerate carbon particles, soluble organic fraction (SOF) that can condense on the surface of the carbon particles or nucleate to form new very small particle during the dilution and cooling process, lesser amounts of sulfate compounds, and other species [7-10]. The particle size distributions are generally lognormal in form and may include three modes

denoted as nucleation, accumulation and coarse modes. Biodiesel fuels have been widely studied in diesel engines because of their lower sulfur, lower aromatic hydrocarbon and higher oxygen contents. The total particle mass is typically reduced when using biodiesel or biodiesel blends, but changes in particle number distributions can vary from study to study [11-15].

The fuel injection system in a direct injection diesel engine is designed to achieve a high degree of atomization with improved fuel penetration, in order to more fully utilize the charge air, to promote the rapid evaporation and ultimately to achieve higher combustion efficiency. The fuel injection pressure (IP) in a standard diesel engine is in the range of 200 to 1700 bar depending on the engine size and type of combustion system employed [16]. Fuel penetration distance increases, mixture formation improves, and combustion duration becomes shorter as injection pressure is increased [17]. Various investigators have reported on the effects of IP on engine performance and exhaust emissions [17, 18].

The aim of this investigation was to study the effect of injection pressure on combustion characteristics, nanoparticles and gaseous emissions from a high speed direct injection (HSDI) diesel engine fueled with ultra-low sulfur diesel (ULSD) and rapeseed methyl esters (RME), for a single injection strategy at a constant start of injection timing of -9 ATDC, at a constant engine speed of 1500 rpm. The injection pressure was varied from 800 bar to 1200 bar, for two engine loads of 2.5 and 5 bar BMEP.

2. METHODOLGY

2.1. Experimental setup

Experiments were carried out in a 2.0 litre, 4 cylinder, 16 valve direct Injection Ford Duratorq (Puma) Euro3 diesel engine, with a compression ratio of 18.2:1. The engine was supplied by Ford as a prototype of a production unit which powered Ford Transits and Mondeo cars. The engine is fully instrumented and coupled to a Schenck eddy current dynamometer. In this investigation, the engine was operated under naturally aspirated mode without EGR. Instrumentation enables the measurement of in-cylinder pressure and exhaust gas emissions under steady-state engine operating conditions. The in-cylinder pressures were measured using a Kistler pressure transducer fitted into the first cylinder of the engine. The signal from the pressure transducer was passed through a charge amplifier and then recorded by the (LabView) software in conjunction with the shaft encoder, enabling pressure data to be logged every 0.125 degrees CA. In-cylinder pressure data were collected over 100 engine cycles per measurement, and the measurement was repeated 5 times for each point in the experimental matrix. These data were averaged from 100 cycles.

The engine has a common rail fuel injection system, with each injector having six holes of 0.154 mm diameter, forming a spray-cone angle of 154°. Engine management software (Gredi) was used to control and change engine running parameters by programming the ECU in real time; injection timing and pressure could be directly adjusted. The gaseous exhaust emissions were acquired using a Horiba-Mexa 7170DEGR gas analyzer. A non-dispersive infrared method was used to measure CO, NO_x emissions were measured via chemiluminescence, and total un-burnt hydrocarbons (THC) were measured using the flame ionization detection technique. The engine exhaust smoke emissions were measured using the AVL–415 smoke meter. The diesel fuel consumption was measured using an AVL fuel consumption meter, which is based on the gravimetric measurement principle.

Measurements were carried out using the standard low sulphur diesel fuel USLD and pure rapeseed methyl ester (RME) was provided by Shell Global Solutions. Table 1 presents the properties of the fuels used in this work.

Table 1.
Fuel properties

Fuel analysis	**Diesel (ULSD)**	**Biodiesel (RME)**
Chemical formula	$C_{14}H_{26.18}$	$C_{18.96}H_{35.29}O_2$
Cetane number	53.9	54.7
Density at 15_C (kg/m3)	827.1	882.54
Viscosity at 40 _C (cSt)	2.467	4.478
LCV (MJ/kg)	43.3	37.4
Sulphur (mg/kg)	10	5
Total aromatics (wt%)	24.4	-
C (wt%)	86.44	77.12
H (wt%)	13.56	12.04
O (wt%)	0	10.84

An electrostatic mobility spectrometer (EMS) was used in this experiment to obtain the exhaust soot particle number size distribution. It is capable of measuring particle mobility diameters in the range from 5 nm to 700 nm. Dilution ratio was kept constant at 31.5.

The data obtained from the experiments conducted were collected from using the instrumentation automation software package LabView. Data batches collected were migrated to Matlab in order to process the data to obtain related values for peak pressure and the accompanying angle at which peak pressure occurred, the angle between start of combustion (SOC) and peak pressure, and to estimate the apparent heat release rate (AHRR). The mathematical processing was carried out using an elementary methodology employing the conventional first law heat release model, assuming a constant specific heat ratio of 1.35 without any accompanying modeling of heat transfer or crevice effects.

The following points list the combustion criteria calculated from the AHRR curve:

1. Start of injection (SOI): this factor was defined from the instructed SOI set within the engine management software. Any impending difference between the instructed and actual SOI is possible due to solenoid delay and should be uniform in

conducted measurements as the engine speed was maintained constant.

2. Ignition delay (ID): the value of ID is defined as the difference between the instructed SOI and calculated SOC.

3. Start of combustion (SOC): the start of combustion is defined as the point at which the heat release rate becomes positive. On the AHRR curve, it is defined as the point where the curve crosses the x-axis.

4. Premixed burn Fraction (PMBF): the value for this factor is calculated from dividing the Integral of the AHRR curve between SOC and EOPMB by the Integral of the AHRR curve between SOC and EOC.

5. End of premix burn (EOPMB): the end of premix burn is defined as the first point at which the second derivative of the AHRR reaches a local maximum following a global minimum. In most conditions, the value of this factor approximates the one that corresponds to the position at which the AHRR curve reaches its first local minimum after a global maximum. But in this study, the second differential was used instead due to the reason of unclear local minimum in the AHRR curve under low load conditions .

6. End of combustion (EOC): this point can be defined as the first point at which the moving average of heat release rate drops below zero.

3. RESLUTS AND DISCUSSION

3.1 Combustion characteristics

Figures (1) and (2) show the variations of the in-cylinder pressure with crank angle at high and low loads with an injection timing of -9 ATDC for RME and ULSD fuels. It can be seen that as the fuel injection pressure increases from 800 bar to 1200 bar the combustion starts earlier. In addition, the in-cylinder pressure peak increases with higher fuel injection pressure. Also note the shift in the location of pressure peaks. The rise in the momentum of the fuel spray leads to better entrainment of air into the core of the fuel spray. In addition to this, high injection pressure provides more energy to break up liquid fuels into smaller droplets, leading to faster evaporation at the periphery of the fuel sprays and faster ignition of the fuel vapour. It can be seen that the RME pressure curves rise earlier, as do the heat release rate plots depicted in Figures (3) and (4); this trend is reflected in the ignition delay (ID) data presented in Figure (5), which indicates that the ID of RME was always shorter than that of ULSD.

The shorter ID of biodiesel is expected, as it is generally (although not universally) the case that biodiesel has a higher cetane number than diesel. This is primarily on account of the lower aromatic content of biodiesel, as well as its longer average chain length. However, biodiesel cetane number depends upon the feedstock from which it is derived; more highly unsaturated feedstocks will tend to produce lower cetane number biodiesels. This is because unsaturation inhibits the alkylperoxy isomerisation reactions which are involved in the kinetic pathways to low temperature chain branching [19].

Although the chemical component of ID is likely to be shorter when fuelling with biodiesel, other properties including increased density, viscosity, surface tension, and boiling point are likely to slightly extend the physical component of ID (but not by a magnitude sufficient to offset the chemical reduction).

At higher operating temperatures the effect of physical properties differences between the two types of fuels will be reduced (viscosity, density, heat capacity, and surface tension, vapor pressure, etc.,) which may explain the larger reduction in biodiesel ID with increasing load.

It can be seen that the ignition delay decreases with an increase in the injection pressure. On average, a reduction of about 1 CAD was observed between 800 bar and 1200 bar for both loads. Higher injection pressure causes better mixing which reduces ignition delay.

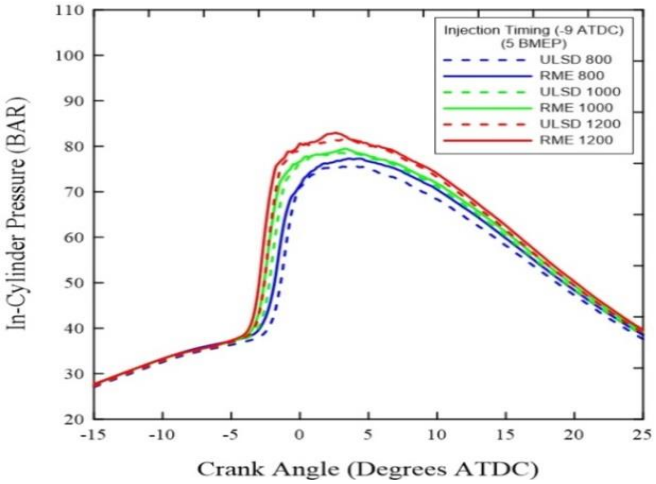

Figure (1) In-cylinder pressure under 80Nm (5 bar BMEP) at different injection pressure

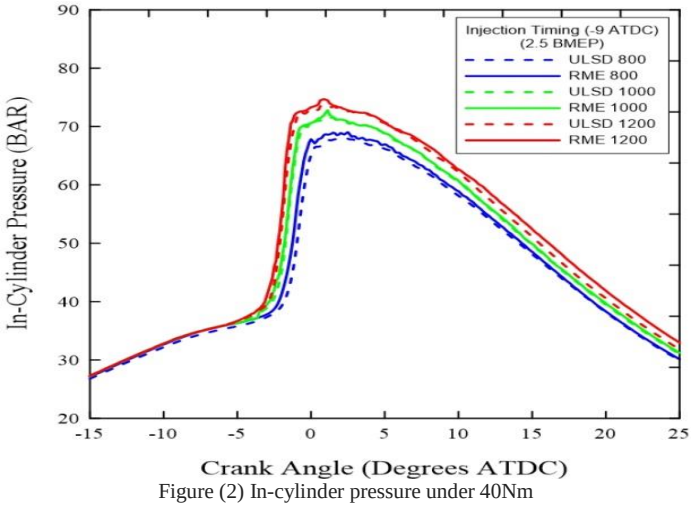

Figure (2) In-cylinder pressure under 40Nm (2.5 bar BMEP) at different injection pressure

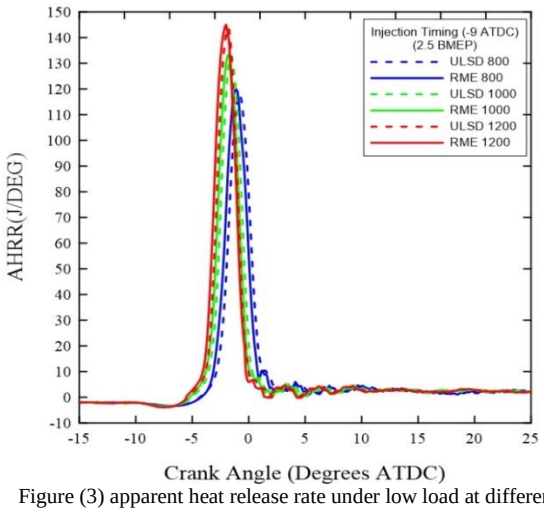

Figure (3) apparent heat release rate under low load at different injection pressure

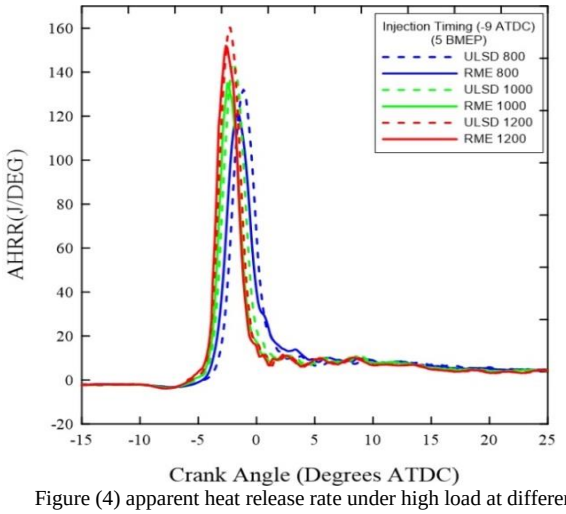

Figure (4) apparent heat release rate under high load at different injection pressure

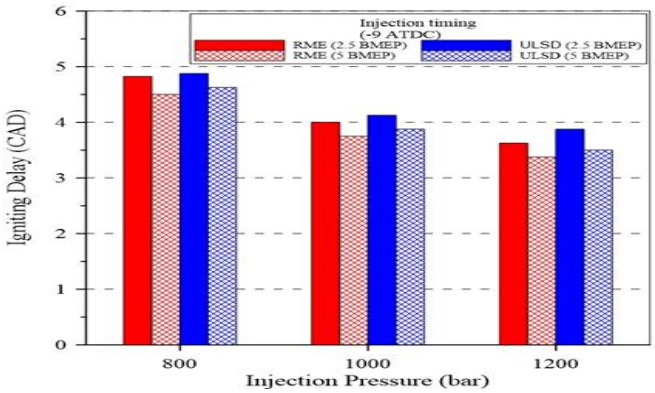

Figure (5) Ignition delay under high and low load at different injection pressure and timing

The peaks of in-cylinder pressure at different injection pressures for both types of fuels at -9 ATDC injection timing are shown in Figure (6), it shows clearly that the peaks of in-cylinder pressure are mostly higher for RME. This is due to the advancement of start of combustion with RME.

The shorter ID of RME leads to a reduction in the premixed burn fraction compared to ULSD, as shown in Figure (7). It can be seen that premixed burn fraction decreases with the increasing of load, due to the increased total heat release required. Hence, duration of diffusion combustion increases with increasing engine load, as shown in Figure (8). A significant difference in diffusion combustion duration between high and low loads was noticed, while there was less variation between the premixed combustion durations. Although the premixed burn duration was shorter, the magnitude of heat that is released during this phase (mass burn fraction) is higher compared to the magnitude of heat that is released in the diffusion phase, as seen in Figure (7). This is a result of the rapid combustion of the premixed fuel–air mixture. Also, a higher oxygen concentration in the spray will result in a reduction in pyrolysis and an increase in oxidation, which may shorten the combustion duration.

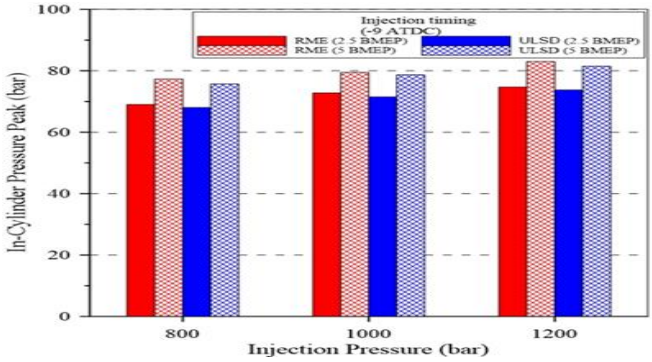

Figure (6) In-cylinder pressure peak at different injection pressure

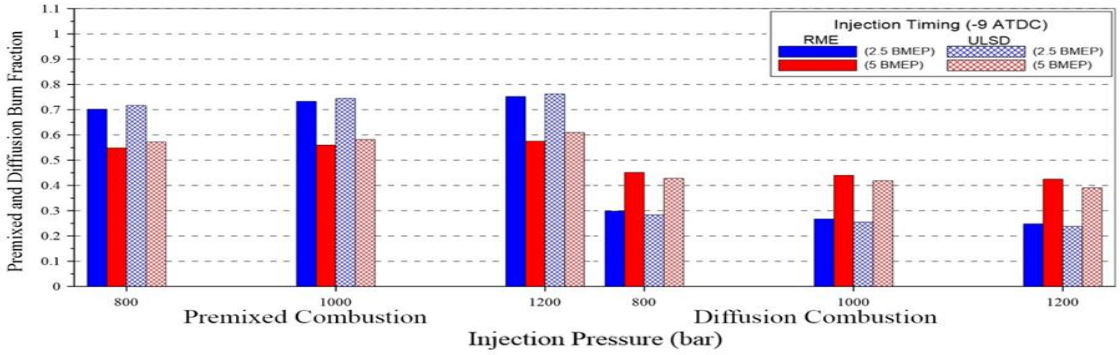

Figure (7) effect of injection pressure on premixed and diffusion burn fraction

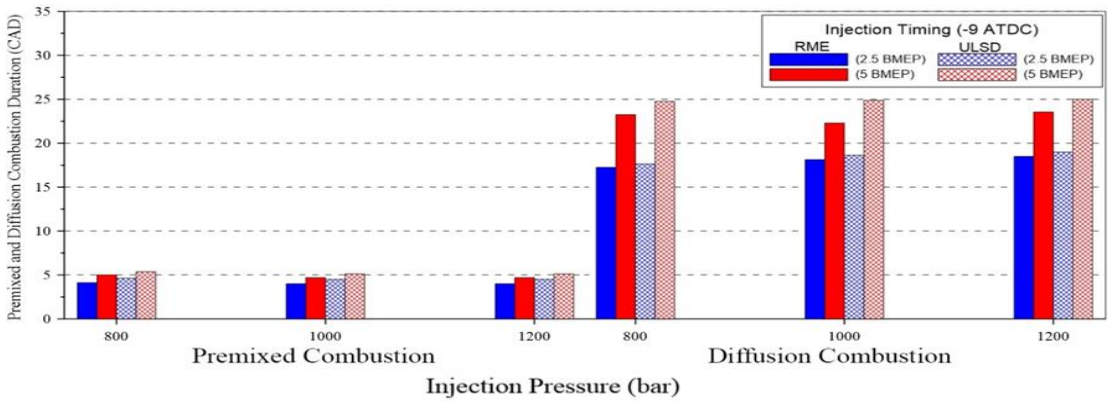

Figure (8) effect of injection pressure on duration of premixed and diffusion combustion

The Brake Specific Fuel Consumption (BSFC) for different injection pressure is shown in figure (9). The minimum BSFC values were obtained with the increased injection pressure, because of improved atomization and mixing. Increasing IP from 800 bar to 1200 bar decreased BSFC values by 19.8% and 3.2% for ULSD at low and high loads respectively, while, the values of decreased were 17.7% and 3.66% for RME at low and high loads respectively. Lapuerta et al. [20] reported that about 98% of the studies they had reviewed reported an increase of BSFC when using biodiesel. The increase in BSFC is mainly associated with the lower heating value of biodiesel compared with that of ULSD. The increase in BSFC at low load is a result of the incomplete combustion of fuel.

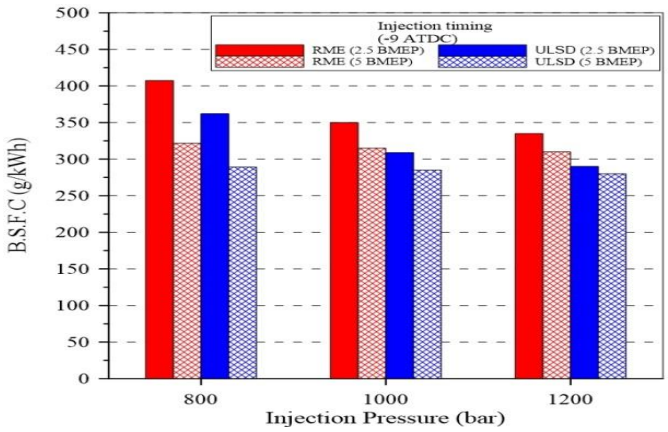

Figure (9) Effect of injection pressure on The Brake Specific Fuel Consumption (BSFC) under high and low load

3.2 Emission characteristics

3.2.1 Nitrogen oxides

Figure (10) shows the effect of fuel injection pressure at high and low loads for both types of fuels at -9ATDC injection timing. It can be seen that an increase in the fuel injection pressure leads to higher NO_x emissions. The premixed burn fraction increases with increased injection pressure, which leads to faster heat release and therefore increased in-cylinder temperatures. The highest cylinder temperature occurs during the premixed combustion phase where the formation of NO_x is dominant. As can be seen in figure (8), the duration of combustion slightly increase with injection pressure increase, that means increasing the in- cylinder temperature which leads to increasing NOx .The difference in NOx emissions between high and low-load is also largely due to differences in in-cylinder temperatures.

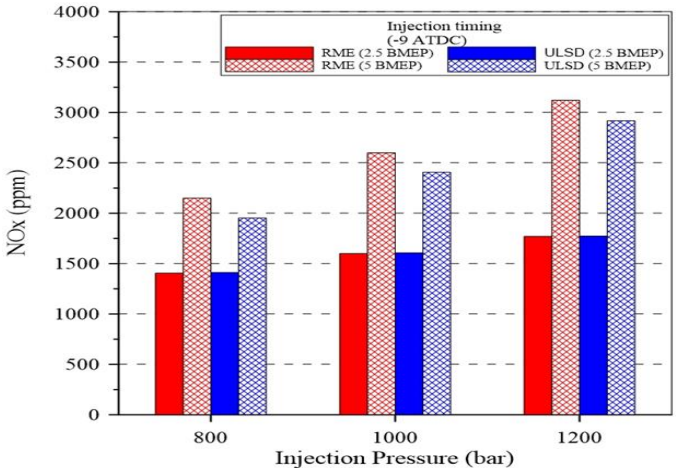

Figure (10) Effect of injection pressure on NO_x emissions under high and low load

At low load (2.5 bar BMEP), the NO_x emissions with USLD are higher than the NO_x emissions with RME, while at high load, the NO_x emissions with RME are higher than the NO_x emissions with USLD. Under most operational conditions, the fuel that combusted most quickly, releasing heat earliest, was the fuel that generated the highest NO_x emissions, as has been observed previously [21]. At low load ULSD had a longer ignition delay (ID) and a larger premixed burn fraction (PMBF), leading to higher combustion temperatures and higher NO_x emissions, in addition, the NOx reduction for biodiesel may be explained by the lower heat of combustion and flame temperatures for biodiesel, which caused a reduction in peak heat release rate and peak combustion temperature under the low load fuel-lean condition. On the other hand, at high load with higher temperatures and greater oxygen availability with RME, fuelling with biodiesel lead to higher NO_x emissions. Premixed combustion, during which in-cylinder pressure and temperature are very high, plays an important role in NO formation .Techniques to control NO_x formation are mainly linked to a reduction in combustion temperature during this phase of combustion. Unfortunately, a reduction in combustion temperature also leads to an increase in soot emissions. The reduction in soot leads to a reduction in soot radiative heat losses; soot radiative heat losses have been

identified as a significant cause of NO_x reduction when operating on traditional petrodiesel, due to the associated temperature reduction [33]. Since in-cylinder soot quantities are lower when fuelling with biodiesel, the magnitude of this temperature reduction may decline, leading to increased temperatures and higher NOx emissions [24]. In addition to increased thermal NO_x due to a reduction in radiative heat losses, it has also been hypothesized that a reduction in soot formation may be chemically associated with increased NOx formation via the prompt NO mechanism [34]. The biodiesel NOx increase may not be driven purely by the Zeldovich mechanism, but may instead be influenced by the fact that during combustion the double bonded molecules found in unsaturated biodiesels could lead to an increase in the quantities of hydrocarbon radicals (CH) in fuel-rich regions, resulting in increased NOx formation via the prompt NO mechanism. Ban-Weiss et al [22] have shown that radiative heat transfer from soot can significantly influence NOx formation in combustion systems. They have been reported that the "cooling effect" of soot radiation may reduce NOx emissions by approximately 25%. For a large PMBF (at low load) , the in-cylinder soot quantities was found that low when fuelling with both ULSD and RME, and therefore the radiative heat losses would be reduced, leading to higher actual temperatures , and the tendency to generate lesser differences in NOx emissions for similar combustion behavior. While, at high load when the PMBF reduced and DBF increased, the in-cylinder soot quantities would be expected to be higher for ULSD than RME, leading to increased heat losses and lower NOx emissions when fuelling with ULSD [21]. Additionally, the oxygen content of biodiesel may reduce the equivalence ratio in fuel-rich regions of the spray, leading to higher adiabatic flame temperatures than petrodiesel [23, 24]. Robbins et al [25] show that the effects of biodiesel usage upon NO_x emissions are inconsistent, varying across engine types, operating modes, fuel compositions, and other parameters. The results reported in this study support that point .

Running on ULSD at high load, an increase of injection pressure from 800 bar to 1000 bar increased NO_x by 23%, and from 800 bar to 1200 bar increased it by 49%; for RME at the same conditions, changing from 800 bar to 1000 bar increased NO_x by 21%, and 800 bar to 1200 bar by 45%. At low load, when making the same changes in injection pressure, NO_x increased by approximately 14% and 25.7% for ULSD, and 13.8% and 25.9% for RME

3.2.2 Smoke number

Figure (11) shows the variations in soot emissions under high and low loads at different injection pressures for both types of fuels. The smoke number at all conditions is lowered by increasing the fuel injection pressure. Higher injection pressure leads to the formation of smaller fuel droplets and faster fuel vaporisation due to better entrainment which eventually results in the reduction of smoke emissions. There is a clear difference in soot emissions between high-load and low-load for all conditions. This difference is related to the large variation in the amount of diffusion combustion (diffusion burn fraction) between high and low-load, as shown in Figure (7), where longer duration of the diffusion combustion phase is associated with higher soot emissions.

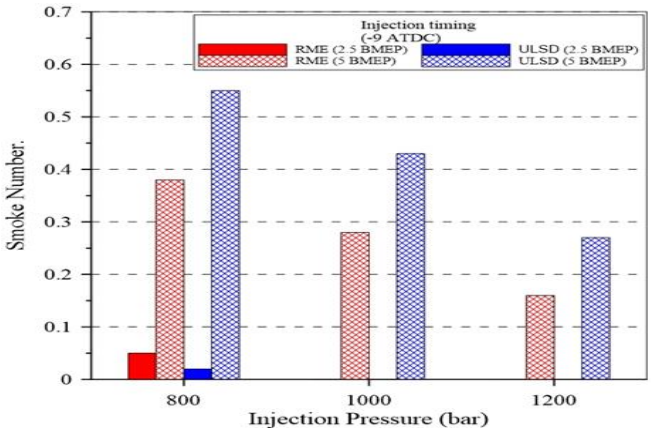

Figure (11) Effect of injection pressure on smoke number under high and low load

It can be seen that the smoke number is reduced to zero under low load at fuel injection pressures of 1000 and 1200 bar, due to the almost completely premixed nature of combustion under these conditions. The smoke numbers of RME were mostly lower than those of USLD, at all conditions. This difference is more readily apparent at high engine loads, because at low load the values for both fuels were very low. The reduction of smoke number with biodiesel can be attributed to the increase of oxygen content in the fuel. The oxygen in the fuel can assist in reducing smoke formation during the stage of diffusion combustion, by reducing the equivalence ratio within the diffusion flame sheath. The improvement is more obvious at high engine loads when a larger percentage of fuel is burned in the diffusion mode, as shown in figure (7). Sooting is reduced when fuelling on biodiesel because of the oxygen content of the fuel and the chemical structure of the hydrocarbons, of which it is composed [21]. The decrease of fuel aromatics of the biodiesel could also lead to a reduction of soot formation, where aromaticity in particular tends to increase the sooting tendency of a fuel [26]. The absence of aromatics in biodiesel, therefore has a direct effect on the soot inception process.

3.2.3 CO and THC emissions

Figures (12) and (13) show the variation of CO and THC emissions at different fuel injection pressures at -9 ATDC for both types of fuels under high and low loads. In figure (12) it can be seen that when fuel injection pressure increases CO emissions decrease. Figure (13) shows the variation of THC emissions with fuel injection pressure. THC emissions decrease with higher fuel injection pressure. Thus, the general emission trends for both THC and CO are similar. Both CO and THC emissions are the products of incomplete combustion, which higher injection pressures tend to discourage. Unburnt hydrocarbon emissions are generally formed as a result of flame quenching. The formation of higher CO and THC emissions are strongly related to the physical properties of the fuel, since factors like viscosity, density, surface tension, vapor pressure, etc., affect spray penetration. If these properties change in a manner that increases spray penetration (as with biodiesel), then increased wetting of the cylinder walls may occur, leading to the formation of higher CO and THC emissions by incomplete combustion.

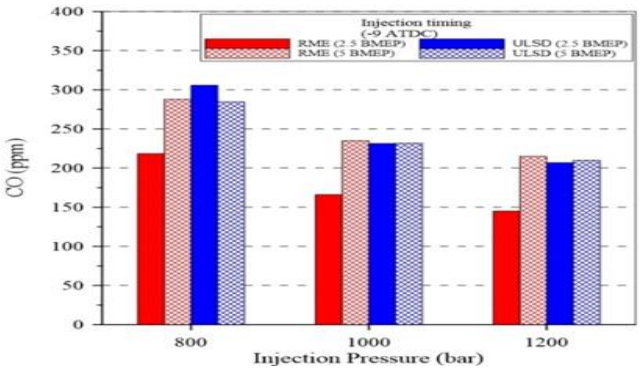

Figure (12) Effect of injection pressure on carbon monoxide emissions under high and low load

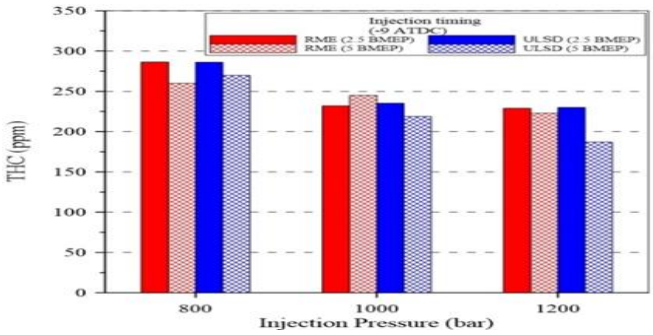

Figure (13) Effect of injection pressure on (THC) emissions under high and low load

3.2.4 Nanoparticles emissions

The effect of injection pressure on the particle number size distribution for ULSD at low load is shown in figure (14). The particle number size distribution shows unimodal log-normal distribution with most of the measured particles lying in the 5-100 nm diameter range. There is a shifting of the curves downwards with increasing injection pressure in a diameter range from 5 nm to 40 nm (nucleation mode), indicating a decrease of these submicron particles with injection pressure. The nucleation mode peak was observed at 22 nm at injection pressures of 800 bar and 1000 bar, while it was reduced to 15 nm at an injection pressure of 1200 bar. It appears that the effect of increased injection pressure on accumulation mode particles is more pronounced than that on the smaller nucleation mode particles; that is, the accumulation mode particles were more significantly reduced in number by increased injection pressure. The premixed burn fraction was increased with injection pressure increase as shown in figure (7), which retards the soot formation process inhibiting the growth and coagulation of small particles and form of larger ones. The increase in fuel injection pressure yields better fuel atomisation by increasing the number and shifting the fuel droplets to smaller sizes, this will improve the combustion process which reduces the emissions of large particles in accumulation mode. It is generally recognized that the key component of accumulation mode particle are chains or clusters of primary-particles ('spherules'), which are formed by the coalescence and growth of particles generated by the nucleation of the products of incomplete combustion. Their size and number concentration can be effected by combustion, oxidation, coagulation and the quantities of aromatic hydrocarbons in the fuel, which serve as direct precursors for carbon particles [27]. At high loads, more fuel is consumed in the diffusion mode and hence more particles are formed. With an increase in the number of particles, the coagulation rate increases and hence larger particles are formed, leading to an increase of particle diameter as shown in Figure (15).

The same behavior can be seen for biodiesel as seen in Figures (16) and (17); at low load the nucleation mode peak was observed at 18 nm for injection pressures of 800 bar and 1000 bar, but was reduced to 15 nm at an injection pressure of 1200 bar. At high load, the nucleation mode peak was observed at 18 nm for an injection pressure of 800 bar, and was reduced to 10 nm at injection pressures of 1000 bar and 1200 bar. The main components of nucleation mode particles are semi-volatile hydrocarbons, sulfate and semi-volatile sulfuric acid, produced from sulfur in fuel.

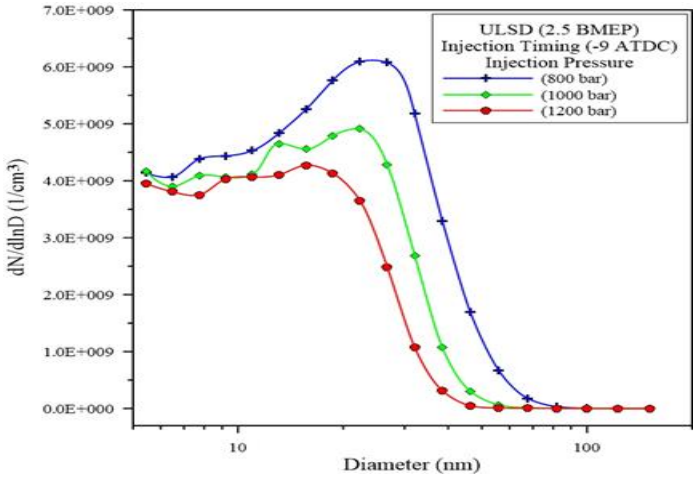

Figure (14) particulate number concentration and size distribution for ULSD at low load

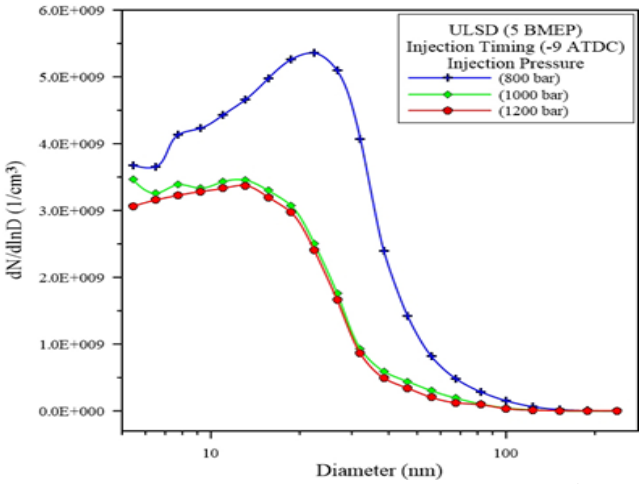

Figure (15) particulate number concentration and size distribution for ULSD at high load

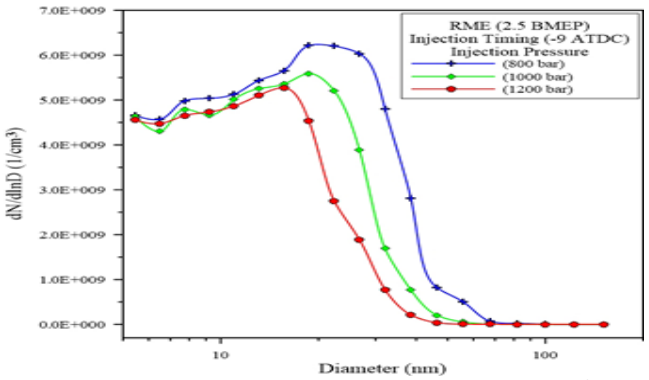

Figure (16) particulate number concentration and size distribution for RME at low load

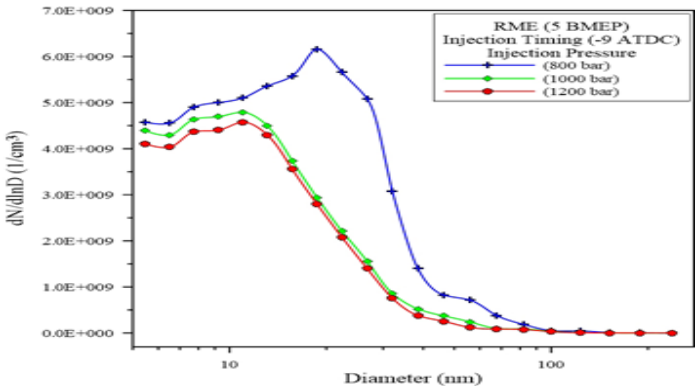

Figure (17) particulate number concentration and size distribution for RME at high load

In Figures (18) and (19) the smaller nucleation particle numbers are shown to be higher for RME at all engine operating conditions, while accumulation mode particles are higher for ULSD . Three mechanisms could lead to greater formation of nucleation mode particles with biodiesel: first, biodiesel reduces soot emissions and therefore, because the availability of solid soot surface is reduced, and the potential for soluble organic fraction (SOF) condensation and adsorption on the soot particles is limited, so high super-saturation may lead to the formation of new particles by nucleation [28]. Second, the increased viscosity and lower volatility of biodiesel could lead to inferior evaporation and air mixing within certain regions of the combustion chamber, possibly causing an increase in the SOF, which would lead to an increase in the quantity of nucleation mode particles generated. Third, the oxygen content of biodiesel causes a reduction in the size of carbonaceous particles, from fine to ultrafine or nanoparticle size categories, which may also result in an increase of nucleation mode particles. Similar results were reported in [11,27-29], where it was shown that the use of biodiesel and blends resulted in higher nucleation mode particle number concentrations than ULSD, whilst giving lower accumulation mode particle concentrations, especially at high engine load. Other researchers [30-32] have shown different results: for instance, Gill et al [30] showed that all oxygenated fuels gave a lower particle number and mass concentration with a shift in the size distribution to smaller mean diameter particles. The reason for a significantly reduced mean particle size can be explained by not only a reduction in the soot formation (i.e. due to increased in-cylinder temperatures and reduced local equivalence ratios) but also by the reduced frequency of particle-particle collisions. The control of the latter can prevent the formation of larger particles through agglomeration as the combustion gases cool. Therefore, with both oxygen enrichment and reduced carbon content in the fuel blends, there is a greater possibility for the oxidation of primary particles. As the number of particles and the rate of agglomeration decrease, the correspondingly smaller particles will lead to a decrease in mean diameter. They found that the quantity of particles smaller than 40 nm is lower with RME, compared to ULSD.

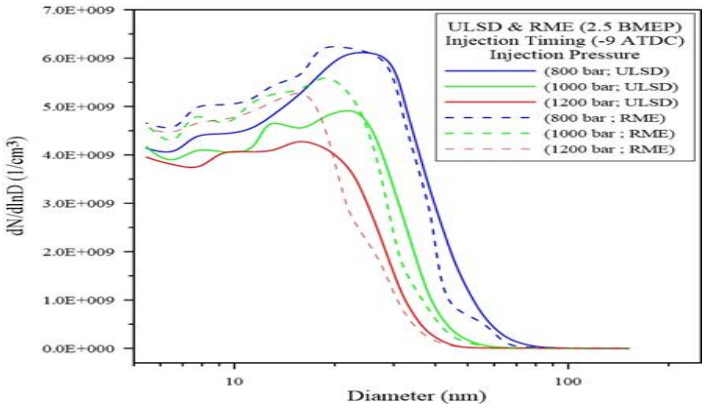

Figure (18) particulate number concentration and size distribution for RME and ULSD at low load

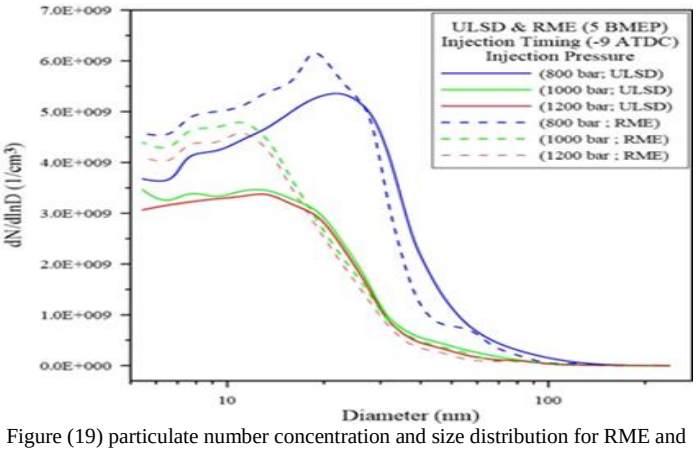

Figure (19) particulate number concentration and size distribution for RME and ULSD at high load

4- Conclusions

1. At all measured conditions, ULSD had a longer ignition delay and a larger premixed burn fraction than RME. This will advance the start of combustion for RME. The ignition delay declined with increasing injection pressure. A shorter ignition delay at high injection pressure also advanced the combustion, and increased the in-cylinder pressure, heat release rate and the maximum values of both.

2.The increased PMBF with increased injection pressure leads to higher in-cylinder temperatures and thus higher NO_x emissions and reduced soot emissions for both types of fuel.

3. The NO_x emissions from RME were lower than those from ULSD under the lower load, but at the higher load RME generated higher NO_x emissions at all injection pressures.

4. The diffusion burn fraction was large at high load for both types of fuels, which led to a significant increase in soot emissions compared to those at low load. Sooting is reduced when fuelling on biodiesel because of the oxygen content of the fuel and the chemical structure of the RME molecules.

5. A clear emission of soot under low load and high fuel injection pressure (1000, 1200) bar is due to the low temperature combustion and the almost completely premixed nature of combustion under these conditions .

6. CO and THC emissions are formed as a result of incomplete combustion, so CO and THC emissions decreased with increasing fuel injection pressure.

7. The minimum BSFC values were obtained at the highest injection pressure, because of improved atomization and mixing efficiency. The BSFC for RME was higher than that of ULSD at all conditions, due to the lower heating value of the biodiesel.

8. The particle number size distribution of the engine shows unimodal lognormal distribution and most of the measured particles are in the range of 5- 100 nm in diameter.

9. Increasing the injection pressure has a more significant effect on the number of accumulation mode particles than it does on the smaller nucleation mode range.

10. The nucleation particle numbers measured were higher for RME than ULSD at all engine operating conditions, whereas accumulation mode particles were more numerous for ULSD than RME.

NOMENCLATURE

AHRR	Apparent Heat Release Rate
ATDC	After Top Dead Centre
BMAP	Brake Mean Effective Pressure
BSFC	Brake Specific Fuel Consumption
CO	Carbon monoxide
C_p	Specific heat at constant pressure
C_v	Specific heat at constant volume
CAD	Crank Angle Degree
DBF	Diffusion burn fraction
ECU	Electronic Control Unit
EGR	Exhaust Gas Recirculation
EOC	End of Combustion
EMS	Electrostatic Mobility Spectrometer
HSDI	High speed direct injection
ID	Ignition delay
IP	Injection Pressure
NO_x	Nitric oxides
PM	Particulate matter
PMBF	Premixed burn fraction
RME	Rapeseed Methyl Ester
SOC	Start of Combustion
SOF	Soluble Organic Fraction
SN	Smoke Number
THC	Total hydrocarbons
ULSD	Ultra-Low Sulfur Diesel Fuel

ACKNOWLEDGMETS

The experimental work of this research has been conducted in the Centre for Advanced Powertrain and Fuels Research (CAPF), School of Engineering and Design, Brunel University, London, UK. Authors are thankful to center staff and special thank is for technicians Kenneth Antiss, and to colleagues Fanos Christodoulou, David Peirce and N. Alozie for their assistance.

References

1- Pi-qiang Tan , Zhi-yuan Hu , Di-ming Lou a, Zhi-jun Li . Exhaust emissions from a light-duty diesel engine with Jatropha biodiesel fuel. Energy 39 (2012) 356- 362

2- Knothe G. Biodiesel and renewable diesel: a comparison. Prog Energy Combust .Sci 2010;36:364–73.

3- Varuvel EG, Mrad N, Tazerout M, Aloui F. Experimental analysis of biofuel as an alternative fuel for diesel engines. Appl Energy 2012;94:224–31.

4- Dwivedi G. , Jain S., Sharma M.P . Impact analysis of biodiesel on engine performance—A review . Renewable and Sustainable Energy Reviews 15 (2011) 4633– 4641.

5- Yage Di , C.S. Cheung , Zuohua Huang . Experimental investigation on regulated and unregulated emissions of a diesel engine fueled with ultra-low sulfur diesel fuel blended with biodiesel from waste cooking oil. SCIENCE OF THE TOTAL ENVIRONMENT 407 (2009) 835 – 846.

6- S. Kent Hoekman , Curtis Robbins. Review of the effects of biodiesel on NOx emissions. Fuel Processing Technology 96 (2012) 237–249.

7- Pi-qiang Tan, Di-ming Lou and Zhi-yuan Hu. Nucleation Mode Particle Emissions from a Diesel Engine with Biodiesel and Petroleum Diesel Fuels. SAE Paper 2010-01-0787.

8- Kittelson D B. Engine and Nanoparticles: A Review. Journal of Aerosol Science, 1998, 29: 575-588.

9- Johnson, T. V. "Diesel Emission Control in Review," SAE Paper 2006-01-0030 .

10- M. Tinsdale , Phil Price and Rui Chen. The Impact of Biodiesel on Particle Number, Size and Mass Emissions from a Euro4 Diesel Vehicle . SAE Paper 2010-01-0796.

11- Lei Zhu, Wugao Zhang, Wei Liu, Zhen Huang. Experimental study on particulate and NOx emissions of a diesel engine fueled with ultra-low sulfur diesel, RME-diesel blends and PME-diesel blends. Science of the Total Environment 408 (2010) 1050–1058.

12- Lei Zhu , C.S. Cheung , W.G. Zhang , Zhen Huang. Effect of charge dilution on gaseous and particulate emissions from a diesel engine fueled with biodiesel and biodiesel blended with methanol and ethanol. Applied Thermal Engineering 31 (2011) 2271-2278.

13- Li-Hao Younga , Yi-Jyun Lioua, Man-Ting Chengb, Jau-Huai Luc, Hsi-Hsien Yangd, Ying I. Tsaie, Lin-Chi Wangf, Chung-Bang Cheng, Jim-Shoung Lai . Effects of biodiesel, engine load and diesel particulate filter on nonvolatile particle number size distributions in heavy-duty diesel engine exhaust. Journal of Hazardous Materials 199– 200 (2012) 282– 289.

14- E. Sukjit , J.M. Herreros , K.D. Dearn , A. Tsolakis , K. Theinnoi. Effect of hydrogen on butanol- biodiesel blends in compression ignition engines. International journal of hydrogen energy 38 (2013) 1624-1635.

15- Pi-qiang Tan , Shuai-shuai Ruan , Zhi-yuan Hu , Di-ming Lou , Hu Li. Particle number emissions from a light-duty diesel engine with biodiesel fuels under transient-state operating conditions. Applied Energy 113 (2014) 22–31.

16- Heywood, J.B., 1988. Internal Combustion Engine Fundamentals. McGraw-Hill Science Engineering.

17- R.A. Bakar, S. Ismail, A.R. Ismail, Fuel injection pressure effect on performance of direct injection diesel engine, American Journal of Applied Science 5 (2008) 197-202.

18- S. Puhan, R. Jegan, K. Balasubbramanian, G. Nagarajan, Effect of injection pressure on performance, emissions, and combustion characteristics of high linolenic linseed oil methyl ester in a DI diesel engine, Renewable Energy 34 (2009) 1227-1233.

19- C.K. Westbrook , W.J. Pitz, S.M. Sarathy, M. Mehl. Detailed chemical kinetic modeling of the effects of CC double bonds on the ignition of biodiesel fuels . Proceedings of the Combustion Institute . 2013,34 (2), 3049-3056.

20- Lapuerta M, Armas O, Jose RF. Effect of biodiesel fuels on diesel engine emissions. Prog Energy Combust 2008 ;34:198–223.

21- D. M. Peirce, N. S. I. Alozie, D. W. Hatherill, and L. C. Ganippa . Premixed Burn Fraction: Its Relation to the Variation in NOx Emissions between Petro- and Biodiesel. Energy Fuels 2013, 27, 3838−3852.

22- Ban-Weiss, G. A.; Chen, J. Y.; Buchholz, B. A.; Dibble, R. W. A numerical investigation into the anomalous slight NOx increase when burning biodiesel; A new (old) theory. Fuel Process. Technol. 2007, 88, 659−667.

23- C.J. Mueller, A.L. Boehman, G.C. Martin, An experimental investigation of the origin of increased NOx emissions when fueling a heavy-duty compression ignition engine with soy biodiesel, SAE International, 2009-01-1792, 2009, pp. 1–28.

24- A.S. Cheng, A. Upatnieks, C.J. Mueller, Investigation of the impact of biodiesel fuelling on NOx emissions using an optical direct injection diesel engine, International Journal of Engine Research 7 (2006) 297–318.

25- C. Robbins, S.K. Hoekman, E. Ceniceros, M. Natarajan, Effects of biodiesel fuels upon criteria emissions, SAE International, SAE 2011-01-1943; JSAE 20119349,2011.

26- Ladommatos, N.; Rubenstein, P.; Bennett, P. Some effects of molecular structure of single hydrocarbons on sooting tendency. Fuel1996, 75, 114−124.

27- Di Yao, Diming Lou, Zhiyuan Hu and Piqiang Ta Experimental Investigation on Particle Number and Size Distribution of a Common Rail Diesel Engine Fueling with Alternative Blended Diesel Fuels. SAE Paper 2011 (2011–01–0620).

28- Pi-qiang Tan, Di-ming Lou and Zhi-yuan Hu. Nucleation Mode Particle Emissions from a Diesel Engine with Biodiesel and Petroleum Diesel Fuels. SAE Paper 2010 (2010–01–0787).

29- Pi-qiang Tan, Zhi-yuan Hu, Di-ming Lou and Bo Li. Particle Number and Size Distribution from a Diesel Engine with Jatropha Biodiesel Fuel. SAE Paper 2009 (2009–01–2726).

30- S.S. Gill , A. Tsolakis , J.M. Herreros , A.P.E. York. Diesel emissions improvements through the use of biodiesel or oxygenated blending components . Fuel 95 (2012) 578–586.

31- M. Tinsdale , Phil Price and Rui Chen. The Impact of Biodiesel on Particle Number, Size and Mass Emissions from a Euro4 Diesel Vehicle. SAE Paper 2010-01-0796.

32- S. Chuepeng , H. Xu , A. Tsolakis ,M. Wyszynski , Ph. Price . Particulate Matter size distribution in the exhaust gas of a modern diesel Engine fuelled with a biodiesel blend. biomass and bioenergy 35 (2 0 1 1) 4 2 8 0-4 2 8 9.

33- Musculus, M. P. B. Measurements of the influence of soot radiation on in-cylinder temperatures and exhaust NOx in a heavy-duty

DI diesel engine. SAE Technical Paper 2005-01-0925.

34- Ren, Y.; Li, X. Numerical simulation of the soot and NOx formations in a biodiesel-fuelled engine. SAE Technical Paper 2011- 01-1385.